Research progress of low-dimensional perovskites: synthesis, properties and optoelectronic applications*

Xinzhe Min, Pengchen Zhu, Shuai Gu, and Jia Zhu†

National Laboratory of Solid State Microstructures, College of Engineering and Applied Sciences, and Collaborative Innovation Center of Advanced Microstructures, Nanjing University, Nanjing 210093, China

Abstract: The lead halide-based perovskites, for instance, $CH_3NH_3PbX_3$ and $CsPbX_3$ (X = Cl, Br, I), have received a lot of attention. Compared with bulk materials, low-dimensional perovskites have demonstrated a range of unique optical, electrical and mechanical properties, which enable wide applications in solar cells, lasers and other optoelectronic devices. In this paper, we provide a summary of the research progress of the low-dimensional perovskites in recent years, from synthesis methods, basic properties to their optoelectronic applications.

Key words: low-dimensional perovskites; nanoplates; nanowires; quantum dots; solar cells; semiconductor lasers
DOI: 10.1088/1674-4926/38/1/011004 **PACS:** 88.40.H-; 81.07.-b **EEACC:** 4110; 4220

1. Fore word

Perovskite, which can be described by chemical formula ABX_3, has been investigated for more than a century because of a series of sought-after physical properties, such as magnetism and ferroelectricity. However, until recent years, newly discovered lead halide perovskites, representatively $CH_3NH_3PbX_3$ and $CsPbX_3$(X = Cl, Br, I), with excellent optical, electrical and mechanical properties have attracted a lot of attention. Impressive progress has been made in the perovskite-based optoelectronic devices since the organometallic perovskite $CH_3NH_3PbI_3$ was first applied for photovoltaic cells in 2009[1]. As is shown in Fig. 1(a), after initial 3.8% achieved at the beginning, the conversion efficiency of perovskite-based solar cells increased rapidly and reached 22.1% in 2016[2]. It is also found that low-dimensional perovskites such as nanoplates (2D), nanowires (1D) and quantum dots (0D) offer various unique advantages, including highly-tunable band gap, excellent mechanical properties[3−5], therefore can serve as promising building blocks for various applications such as photovoltaic and light emitting devices.

2. Introduction

2.1. Perovskites

As is shown in Fig. 1(b), the lead halide perovskites with formula ABX_3 typically have unit cells composed of five atoms in a cubic structure (α phase). Typically, cation A is $CH_3NH_3^+$ or Cs^+, which has twelve nearest anions X, while B is Pb^{2+}, and forms into an octahedral with 6 nearest anions X. X is a kind of halogen with a radius similar to A, together with cation A and B constituting a cubic closepacked structure.

The most heavily investigated perovskite is organic-inorganic hybrid $CH_3NH_3PbX_3$ (X = Cl, Br, I) due to its high light absorption coefficient and long carrier lifetimes. Recently, inorganic perovskite $CsPbX_3$ is also attracting a lot of attention because of excellent luminescence and stability.

2.2. Low-dimensional perovskites

Low-dimensional perovskites generally can be divided into three categories: quantum dots (zero dimension), nanowires (one dimension) and nanoplates (two dimensions).

As shown in Fig. 2, the two-dimensional perovskites have one dimension confined at nanoscale, thus electrons can only move in the other two directions.

The one-dimensional perovskites possess several common morphologies such as nanowires, nanorods and nanotubes[7−11], Its basic structure is shown in Fig. 3.

The zero-dimensional perovskite materials, often called quantum dots, are a batch of tiny particles containing several dozens of atoms, which is shown in Fig. 4. After the surface modification, these particles can be combined with unique optical, electrical properties. The band gap of zero-dimensional perovskite is highly tunable, particularly beneficial for LEDs as well as solar cells[12−15].

Compared with bulk perovskites, the emitting wavelength of low-dimensional perovskites is highly tunable. In 2015, H. Huang *et al*.[16] utilized temperature to exert control over the size and therefore the bandgap of perovskite $CH_3NH_3PbBr_3$ quantum dots. They injected the DMF solution of precursors, long-chain ligands and $CH_3NH_3PbBr_3$ into toluene which was precooled or heated under vigorous stirring to selected set points in the temperature range of 0 to 60 ℃ and found that the radius of the quantum dots decreases when the temperature goes down. $CH_3NH_3PbBr_3$ quantum dots with the range from 1.8 to 3.6 nm are successfully demonstrated with emission peak conveniently tuned in the region of 472–520 nm.

* Project jointly supported by the State Key Program for Basic Research of China (No. 2015CB659300), the National Natural Science Foundation of China (Nos. 11321063, 11574143), the Natural Science Foundation of Jiangsu Province (Nos. BK20150056, BK20151079), the Project Funded by the Priority Academic Program Development of Jiangsu Higher Education Institutions (PAPD), and the Fundamental Research Funds for the Central Universities.

† Corresponding author. Email: jiazhu@nju.edu.cn

Received 23 August 2016, revised manuscript received 9 October 2016

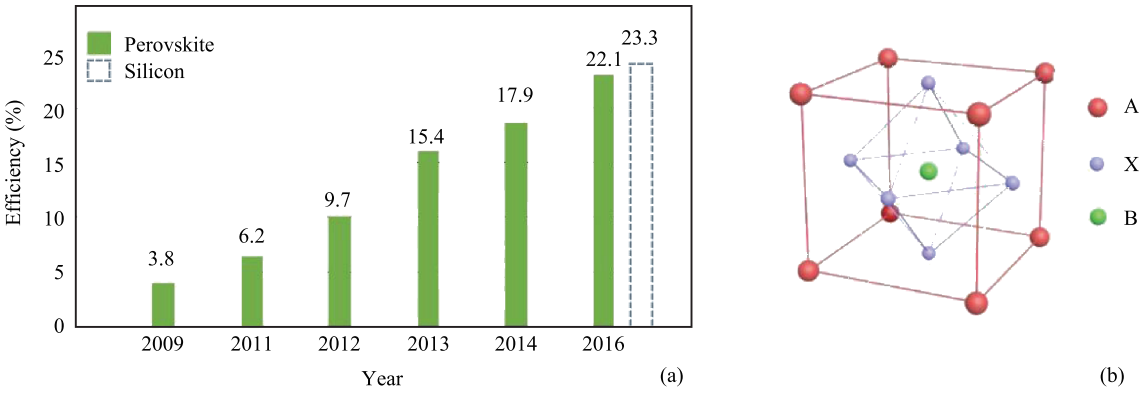

Fig. 1. (Color online) (a) The progress of perovskite solar cells[1, 6]. (b) Crystal structures of perovskites.

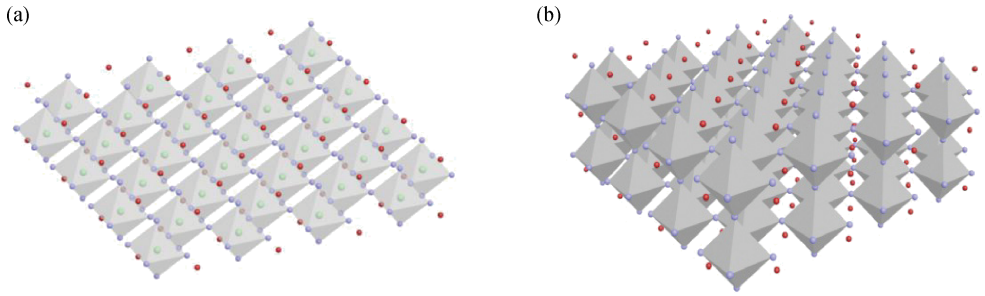

Fig. 2. Perovskite nanoplates. (a) Monolayer. (b) Multilayer.

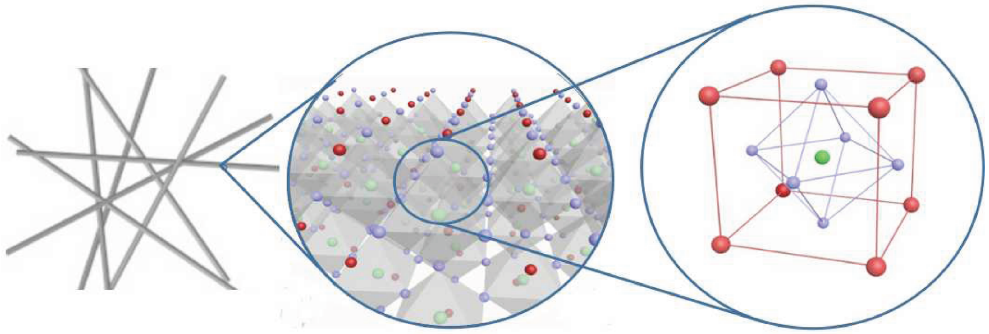

Fig. 3. Perovskite nanowires.

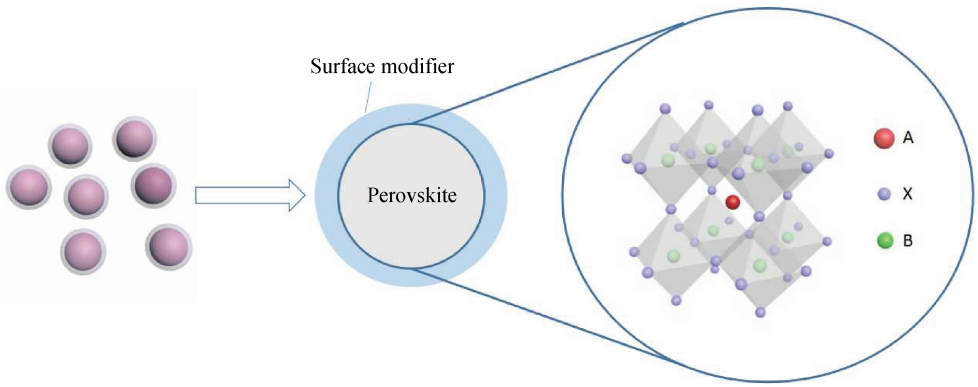

Fig. 4. Perovskite quantum dots.

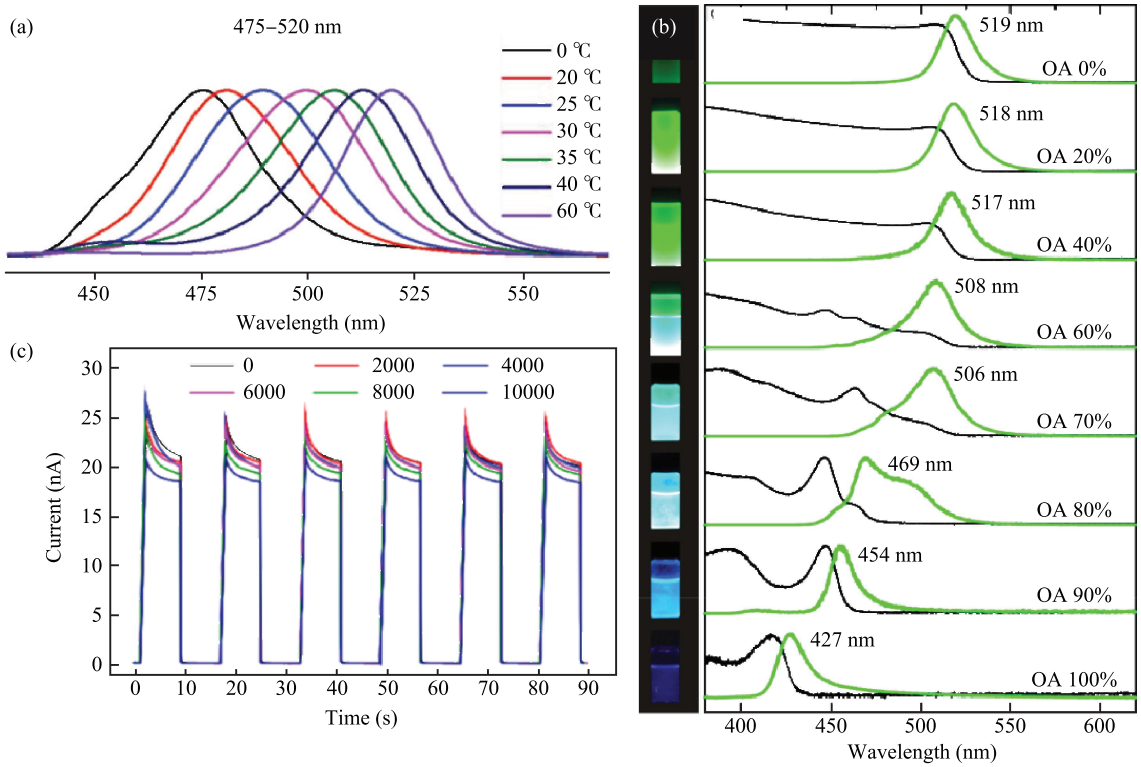

Fig. 5. (Color online) (a) PL spectra tunability of $CH_3NH_3PbBr_3$ PQDs over the range of wavelengths indicated[16]. (b) PL and UV−VIS spectra of perovskite films prepared from the aforementioned suspensions[17]. (c) I–t curves of network PD arrays. The bias voltage was 10 V and the 650 nm light power density was 100 μW/cm^2[18].

When it comes to two-dimensional perovskite, quantum confinement effect can also be observed directly. In 2015, Feldmann *et al*.[17] utilized $CH_3NH_3Br_3$ and $PbBr_2$ to fabricate $CH_3NH_3PbBr_3$ nanoplates with different thickness. They mixed OA and MA, then injected the mixture into the $CH_3NH_3PbBr_3$ solution to tune the number of layers. It is found that when the ratio of OA decreases in the mixture, the thickness of perovskite produced increases. Therefore, perovskites with emission peaks from 427 to 519 nm are demonstrated.

Besides its tunable band gap, low-dimensional perovskite is also well-known for its mechanical flexibility. In October 2015, the $CH_3NH_3PbI_3$ perovskite networkbased photodetectors were fabricated on PET substrates by Deng *et al*.[19] which demonstrate stable performance over a large number of bending. As shown in Fig. 5(c), after 10 000 times of bending at a large angle (∼80°), the photocurrent of the production shrank less than 10%. Song *et al*. reported the fabrication of atomically thin, 2D $CsPbBr_3$ (∼3.3 nm thick) with excellent flexibility in 2016. After bending over 10 000 times, the photocurrent of the device decayed from 2.37 μA in its initial state to 2.31 μA.

3. Material synthesis

3.1. Fabrication of two-dimensional perovskites

Since Geim *et al*.[20] reported graphene in 2004 for the first time, much attention has been paid to 2D layered compounds. As perovskites demonstrate interesting electrical and optical properties such as intrinsic ambipolar transport, high optical absorption coefficient and long carrier diffusion length, a variety of methods have been developed to synthesize 2D perovskite film. In 2014, ultra-thin flakes (∼3 nm) of 2D organic-inorganic perovskite $(C_6H_9C_2H_4NH_3)_2PbI_4$ were successfully produced by Niu *et al*.[21], using the micro-mechanical exfoliation. Xiong and co-workers[22] reported the synthesis of perovskite nanoplates (∼ tens of nanometers) by chemical vapor deposition (CVD) method. Liao *et al*.[23] reported a one-step solution self-assembly method to prepare a single-crystalline square microdisk of $CH_3NH_3PbI_3$ with a thickness of about 500 nm. In 2016, Liu *et al*. showed a combined solution process and vapor-phase conversion method to synthesize 2D hybrid organic−inorganic Perovskite nanoplates. It is found that this high-quality 2D perovskite sample as thin as a single unit cell has a regular shape and exhibits excellent optoelectronic properties as well as tunable photoluminescence.

As shown in Fig. 6, the fabrication of $CH_3NH_3PbI_3$ through a combined solution and vapor-phase conversion method can be divided in two steps. At first, the saturated PbI_2 aqueous solution was cast onto a substrate and subsequently heated from 30 to 80 °C. After the complete evaporation of the solution, 2D PbI_2 nanosheets started to nucleate on the substrate. As the second step, the CH_3NH_3I powder was placed at the center of a CVD furnace to carry out the CVD process while the as-grown 2D PbI_2 nanosheets on the silicon oxide substrate were mounted downstream of the apparatus. After the CVD section, the CH_3NH_3I molecules have intercalated into the interval sites of PbI_6 octahedron layers which formed the 2D $CH_3NH_3PbI_3$ perovskite nanosheets.

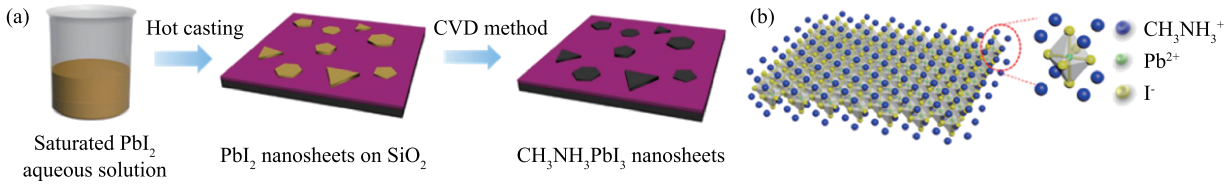

Fig. 6. (Color online) The fabrication of perovskite nanoplates by the combined solution process and vapor-phase conversion method.

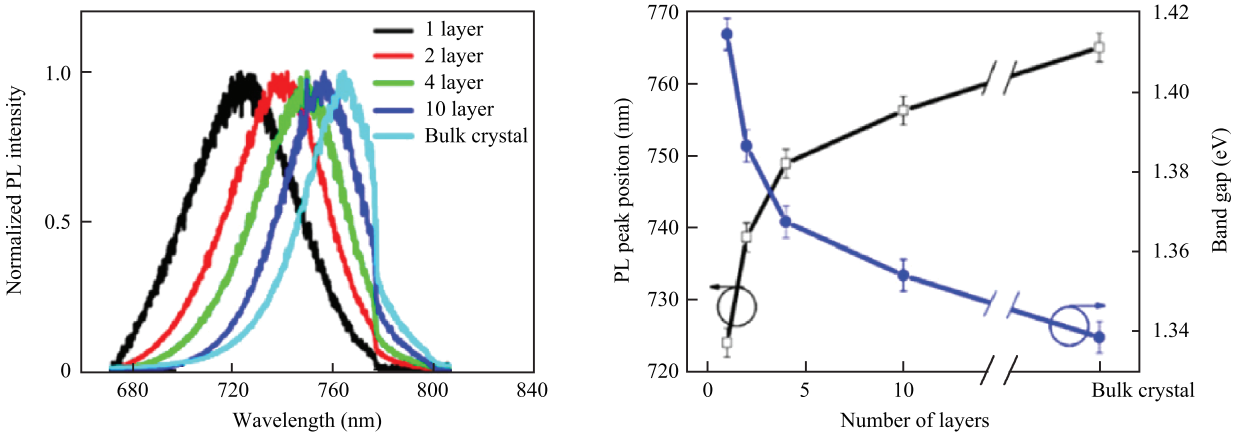

Fig. 7. (Color online) Normalized PL spectra of 2D perovskite nanosheets with different thicknesses[24].

Compared with bulk perovskites, the 2D sheets exhibits high quantum efficiency, together with strong quantum-confinement effect as well. As shown in Fig. 7, the PL peaks shift to shorter wavelength gradually when decreasing the perovskite thickness, while the PL peak of the perovskite with single-unit-cell thickness is located around 720 nm.

3.2. Fabrication of one-dimensional perovskites

In early 2015, perovskite nanowires were fabricated by Deng *et al.*[27] by a one-step solution process. They dropped 10 ml of the precursor solution which was prepared by mixing PbI_2 and CH_3NH_3I onto the preheated substrates and got the $CH_3NH_3PbI_3$ nanowires with the average radius of 500 nm. Meanwhile, Jeong-Hyeok *et al.*[28] reported the fabrication of $CH_3NH_3PbI_3$ nanowires with a radius of about 100 nm, and nanowire-based solar cell efficiency over 14%. Zhang *et al.*[29] synthesized the pure inorganic $CsPbX_3$ nanowires through a catalyst-free, solution-phase method. It is found that cesium oleate can react with lead halide in the presence of oleic acid and oleylamine at 150–250 °C to create the 9–12 nm-diameter CsPbX3 nanowires. It is also found that the morphology and diameter of nanowires can be effectively tuned by changing the temperatures of the reaction.

In 2016, Zhu *et al.*[7] reported a direct path to convert thin film to nanowires. Through a dissolution-recrystallization process, they fabricated $CH_3NH_3PbI_{3-x}Cl_x$ nanowires (diameter ranging from 0.1 to 1 μm) with excellent flexibility and optical properties. As shown in Fig. 8, the whole conversion process can be divided into 3 steps. Firstly, they dissolved the mixtures of $PbCl_2$ and CH_3NH_3I in DMF. The solution is then spin-coated onto a glass substrate, followed by an annealing process, to form a layer of perovskite film. Secondly, a solvent which contains DMF and isopropanol is spin-coated onto the perovskite thin film and it turns out that the perovskite thin film was rapidly dissolved by the mixed solvent because of the great solubility of perovskite in DMF. Finally, the nanowires are formed when the substrates were subsequently spun and heated, as the solution quickly reaches supersaturation during the evaporation and the perovskite nanowires start to grow. It is believed to be a dissolution-recrystallization process. Furthermore, it is found that the density, diameters and size distribution of the nanowires can be easily manipulated by decreasing the concentration of DMF in IPA or increasing the rotation speed of the spin-coater, which offers researchers a convenient and effective way to fabricate perovskite nanowires with desirable properties.

3.3. Fabrication of zero-dimensional perovskites

In 2012, Japanese scientist Kojima *et al.*[31] synthesized the $CH_3NH_3PbBr_3$ quantum dots with porous alumina media for the first time. They reported the nanocrystals with high density and green photoluminescence self-organized within a thin Al_2O_3 film, which was used as the mesoporous medium. However, the size of $CH_3NH_3PbBr_3$ quantum dots mainly depends on the radius of Al_2O_3 pore and could not be controlled effectively, which largely restricted the application.

In 2014, Schmidt *et al.*[32] reported the fabrication of 6-nm-diameter $CH_3NH_3PbBr_3$ quantum dots with a non-template synthesis. Zhang *et al.*[33] demonstrated another method called LARP, through which they successfully synthesized $CH_3NH_3PbBr_3$ quantum dots with great luminescent properties and a diameter less than 5 nm. During the fabrication process, they mixed the CH_3NH_3Br and $PbBr_2$ and dissolved the mixture with n-octylamine and oleic acid in DMF to form a precursor solution. Then, the precursor solution was dropped into toluene with vigorous stirring. The quantum dots which

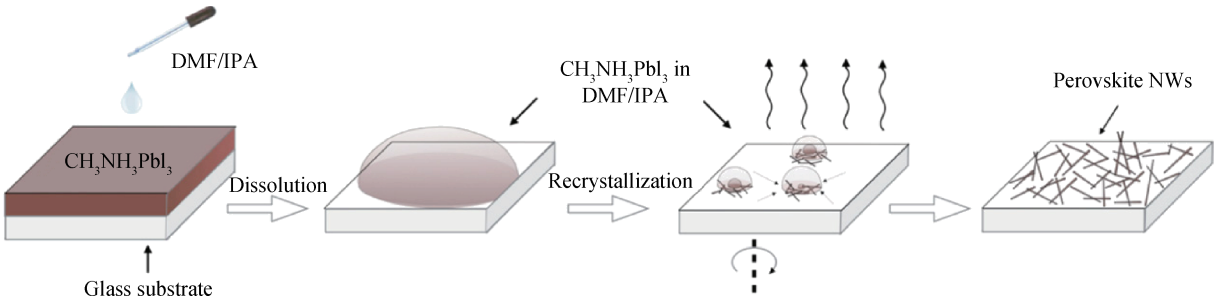

Fig. 8. (Color online) The fabrication of perovskite nanowires by the dissolution-recrystallization process[7].

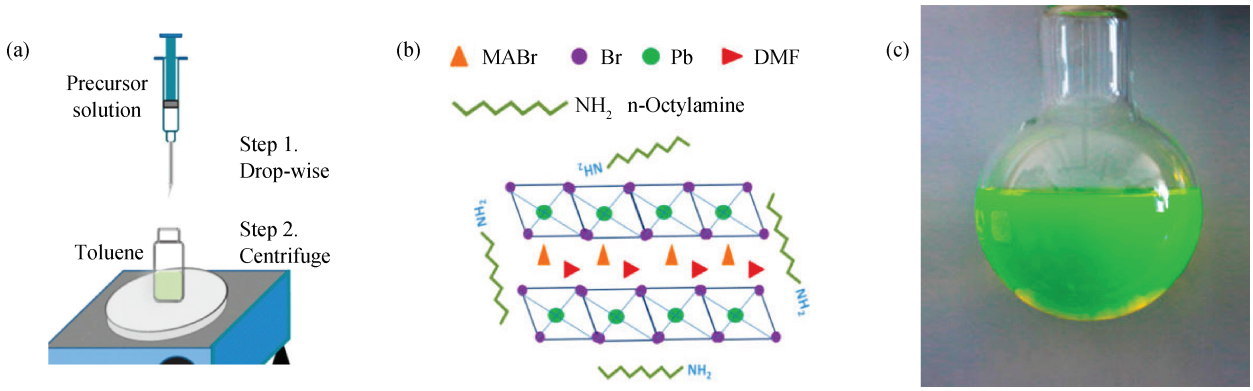

Fig. 9. (Color online) The fabrication of perovskite quantum dots by LARP technique[33].

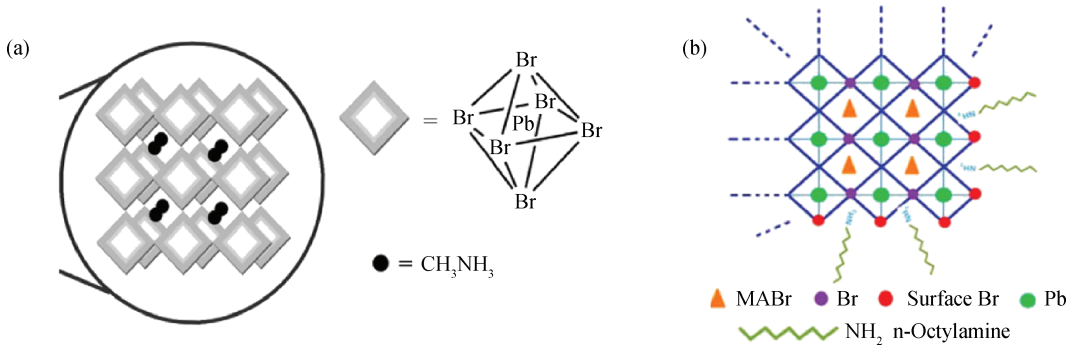

Fig. 10. (Color online) (a) The structure of $CH_3NH_3PbBr_3$ quantum dots[32]. (b) The structure of $CH_3NH_3PbBr_3$ quantum dots after surface modification[33].

can be achieved through a centrifugation has been fabricated during this period. As shown in Fig. 9, the components of the quantum dots can be conveniently tuned from $CH_3NH_3PbCl_3$ to $CH_3NH_3PbI_3$ by varying the precursors and solvents following a similar LARP strategy.

It is found that without n-octylamine added, the precursors undergo fast crystallization and are aggregated into large particles and subsequently precipitated from the solution. The use of other alkylamines with longer chains can also control the crystallization process and produce colloidal QD solutions. Moreover, other long-chain alkyl acids (octanoic acid, butyric acid, etc.) are also suitable to stabilize the formed colloidal $CH_3NH_3PbBr_3$ quantum dots. Based on the observations, it is assumed that the crystallization process is controlled by the supersaturation induced by the solubility change with solvent mixing[33]. After the proper chemical passivation of n-octylamine and oleic acid on the surface, as shown in Fig. 10(b), Zhang gets the quantum dots with uniform diameter (~3.3 nm) and a luminescent efficiency up to 70%.

Huang *et al.*[34] fabricated the $CH_3NH_3PbBr_3$ quantum dots with tunable size and the emission peaks covering the range from 475 to 520 nm. Song *et al.*[35] synthesized the high-quality $CsPbX_3$ quantum dots through hot injecting cesium stearate (CsSt) to $PbBr_2$ solution. These quantum dots have an average diameter of 8 nm as well as good crystallinity, which is preferred for improving the luminescent efficiency and the LED device performance. It is also found that the size of quantum dots can be controlled by the reaction temperature. As the reaction temperature increases, the size of the QDs increases leading to PL peak shifting to longer wavelength.

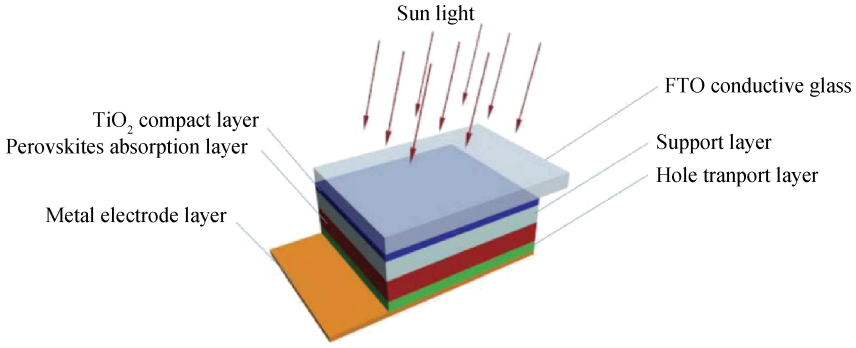

Fig. 11. (Color online) The typical structure of perovskite solar cells.

4. The application of low-dimensional perovskites

Because of these unique properties of low-dimensional perovskites, they have been used for various optoelectronic applications, such as solar cells, LEDs and lasers.

4.1. Perovskite solar cells

The typical structure of perovskite solar cells is shown in Fig. 11, which includes 6 parts-FTO conductive glass, hole transport layer, perovskites absorption layer, support layer, TiO_2 compact layer and metal electrode layer.

When it comes to low-dimensional perovskites, it was found by Smith *et al.*[40] that one kind of 2D perovskites $(PEA)_2(MA)_2[Pb_3I_{10}]$ (PEA = $C_6H_5(CH_2)_2NH_3^+$, MA = $CH_3NH_3^+$) thin films can be used for solar cells with great moisture resistance. As we all know, the perovskite solar cell shows a poor stability to moisture and requires anhydrous processing and operating conditions. The lack of resistance of humidity remains a concern for large-scale device fabrication or their long-term use. When the solar cell is exposed to the humid environment, perovskite molecules will slowly react with water, the chemistry equation of which is shown as follows.

$$CH_3NH_3PbI_3 \overset{H_2O}{\longleftrightarrow} CH_3NH_3I(aq) + PbI_2(aq).$$

In the process, a hydrolytic reaction occurs that loses the MA^+ cation gradually and the perovskite films will decompose to yellow PbI_2 after a short time with a degradation of the solar cells' performance. However, the 2D $(PEA)_2(MA)_2[Pb_3I_{10}]$ films fabricated by Smith *et al*. exhibit extremely high moisture stability which benefits their potential technological exploitation. As the PXRD pattern shows in Fig. 12(a), there are no additional reflections over a period of 46 days of 52%-humidity-level exposure, and their first-generation devices showed an open-circuit voltage of 1.18 V and a power conversion efficiency of 4.73%. In contrast, the new phase is obtained in the pattern of $MAPbI_3$ films, which can be indexed to the PXRD pattern of PbI_2 (Fig. 12(b)).

The moisture-resistant property of the 2D $(PEA)_2(MA)_2[Pb_3I_{10}]$ may be attributed to the hydrophobicity of the long $(PEA)_2(MA)_2$ cation chain and the highly oriented and dense nature of the $(PEA)_2(MA)_2[Pb_3I_{10}]$ films, which

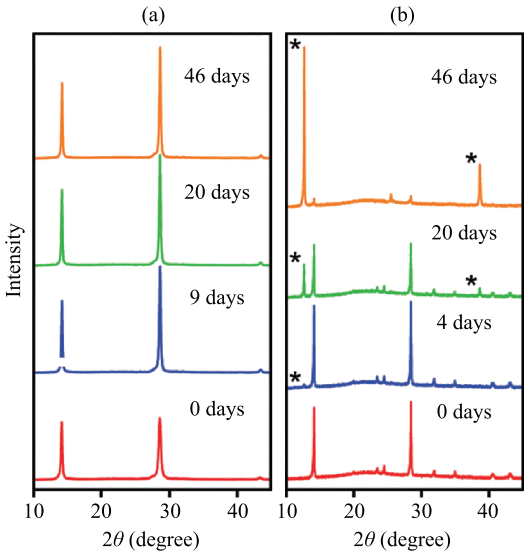

Fig. 12. (Color online) PXRD patterns of films of (a) $(PEA)_2(MA)_2[Pb_3I_{10}]$ and (b) $MAPbI_3$which were exposed to 52% relative humidity.

prevent the direct contact of adventitious water with the $(PEA)_2(MA)_2[Pb_3I_{10}]$.

In 2015, Park *et al.*[41] reported the fabrication of inorganic perovskite solar cells containing $Cs_3Bi_2I_9$ thin films, which have the open-circuit voltage of 0.85 V and power conversion efficiency of 1.09%. Cao and co-workers[42] reported that they had implemented the $(C_4H_9NH_3)_2(CH_3NH_3)_2Pb_3I_{10}$ nano thin film in solid-state solar cells with an initial power conversion efficiency of 4.02% and open-circuit voltage of 929 mV.

As mentioned above, perovskite nanowirebased solar cells have also been demonstrated[28]. $MAPbI_3$ nanowires with the mean diameter of 100 nm were successfully grown with the aid of aprotic solvent DMF in two-step spin coating procedure and the best performing device employing $CH_3NH_3PbI_3$ nanowires delivered photocurrent density of 19.12 mA/cm^2 and voltage of 1.052 V, leading to a power conversion efficiency (PCE) of 14.71%.

4.2. Semiconductor lasers

In 2001, ZnO nanowirebased lasers were demonstrated by Yang and co-workers[45] for the first time. Since then, semiconductor nanowire lasers, owing to their ultracompact

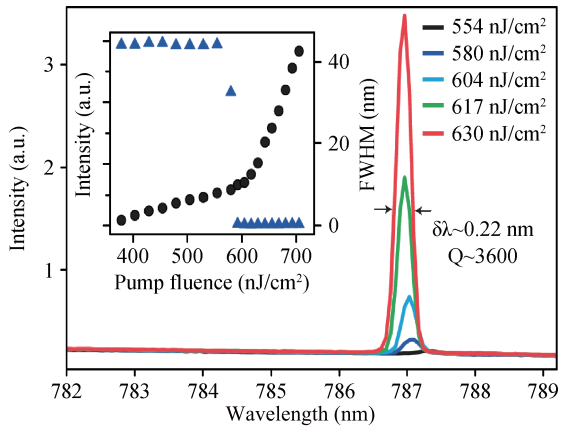

Fig. 13. (Color online) Nanowire emission spectra around the lasing threshold[9].

physical sizes, highly localized coherent output, and efficient waveguiding, are promising building blocks for fully integrated nanoscale photonic and optoelectronic devices. Each nanowire can serve as a waveguide along the axial direction and the two end facets form a Fabry-Perot cavity for optical amplification. However, high lasing threshold not only makes key technical advancement such as electrically driven lasing and integration into optoelectronic devices difficult, but also imposes fundamental limits due to the onset of Auger recombination losses[43, 44]. Researchers turn to lead halide perovskites in search for an ideal material for nanowire lasing. The long carrier lifetimes and diffusion lengths along with high fluorescence yield and wavelength tunability make lead halide perovskites ideal materials for lasing.

Xiong *et al.*[43] reported a room temperature nanolaser based on single-crystal hexagonal phase $FAPbI_3$ nanowires by a low-temperature solution process. Zhu *et al.* developed a surface-initiated solution growth strategy with a lead acetate ($PbAc_2$) solid thin film to produce high-quality single-crystal $CH_3NH_3PbI_3$ nanowires. Despite the low yield, the room-temperature and wavelength-tunable lasing from single-crystal lead halide perovskite nanowires has very low lasing thresholds (220 nJ/cm^2) and high quality factors ($Q \sim 3600$). The lasing threshold corresponds to a charge carrier density as low as 1.5×10^{16} cm^{-3} and the FWHM (full wave at half maximum) of the lasing peak at 787 is 0.22 nm, as shown in Fig. 13. Eaton *et al.*[46] reported the low-temperature, solution-phase growth of cesium lead halide nanowires, exhibiting low-threshold of 5 μJ/cm^2 and the quality factor as high as 1009. Furthermore, lasing of this material under constant, pulsed excitation can be maintained for over 1 h, which demonstrated excellent stability of these inorganic perovskite nanowires as well.

In 2016, Nurmikko *et al.*[47] took an important step toward practically usable two-dimensional perovskite lasers. They demonstrated high degree of temporally and spatially coherent lasing whereby well-defined directional emission near 788 nm wavelength at optical pumping energy density threshold of 68.5 ± 3.0 μJ/cm^2. The measured power conversion efficiency and differential quantum efficiency of the perovskite photonic crystal laser are (13.8 ± 0.8)% and (35.8 ± 5.4)%, respectively.

5. Light-emitting diode devices

More recently, these solution-processed perovskites have also shown their promise in light-emitting diodes (LED). In 2014, Tan *et al.*[48] reported the application of perovskites in LED for the first time. They utilized $CH_3NH_3PbCl_{3-x}I_x$ as the light-emitting layer, emitted the laser with wavelength of 754 nm in near-infrared regions and achieved the external quantum efficiency (EQE) of 0.76%. Less than 2 years later, the EQE of perovskite LED had been increasing rapidly to as high as 8.53%, which was reported by Chao *et al.* As quantum dots including CdSe, CdTe, CdS have shown great performance in LEDs since 1994, perovskite quantum dots have also attracted intensive interest recently. In 2015 Song and co-workers[35] fabricated the LED devices based on inorganic $CsPbX_3$ quantum dots, with emission peaks of 455, 516 and 586 nm, corresponding to $CH_3NH_3PbCl_3$, $CH_3NH_3PbBr_3$ and $CH_3NH_3PbI_3$, respectively.

In 2016, Gong *et al.*[51] demonstrated the $MAPbBr_{3-x}I_x$ LED with the EQE of 4.9%. In the same year, an LED fabricated with $CH_3NH_3PbBr_3$ nanoparticles was reported by Xing *et al.*[52] , of which the EQE is up to 7.84%. Other than quantum dots, two-dimensional perovskites have also been applied to LED since 2015. Yantara *et al.*[53] fabricated the green LED with $CsPbBr_3$ thin films by the end of 2015 with EQE of only 0.008%. Ling *et al.*[54] succeeded in fabricating $CH_3NH_3PbBr_3$ nanoplate-based LED devices with EQE up to 0.038% and improved stability.

6. Summary and prospects

Despite tremendous progress in the past few years, there are still issues that need to be addressed to enable large-scale applications. For example, because of large surface/volume ratio of low dimensional materials, hydrolysis[55] which exists in bulk perovskites as well becomes a serious concern. A common approach is to add a protective layer between perovskite and HTM layer, for example, Al_2O_3 films. Encapsulation is critical for stability as well[56]. With improved scalability of processes and stability of devices, it is expected that this type of low-dimensional perovskite can play a practical role in various optoelectronic applications in the foreseeable future.

References

[1] Kojima A, Teshima K, Shirai Y, et al. Organometal halide perovskites as visible-light sensitizers for photovoltaic cells. J Am Chem Soc, 2009, 131(17): 6050
[2] http://www.nrel.gov/ncpv/images/efficiency_chart.jpg
[3] Dang Y Y, Ju D X, Wang L, et al. Recent progress in the synthesis of hybrid halide perovskite single crystals. Cryst Eng Comm, 2016, 18: 4476
[4] Leyden M R, Jiang Y, Qi Y B. Chemical vapor deposition grown formamidinium perovskite solar modules with high steady state power and thermal stability. Sci Technol Adv Mater, 2015, 16: 036004
[5] Cui J, Yuan H L, Li J P, et al. Recent progress in efficient hybrid lead halide perovskite solar cells. Sci Technol Adv Mater, 2015, 16(3): 036004

[6] Yao X, Ding Y L, Zhang X D. A review of the perovskite solar cells. Acta Phys Sin, 2015, 64(3): 038805
[7] Zhu P C, Gu S, Zhu J, et al. Direct conversion of perovskite thin films into nanowires with kinetic control for flexible optoelectronic devices. Nano Lett, 2016, 16(2): 871
[8] Eatona S W, Lai M L, Gibson N A, et al. Lasing in robust cesium lead halide perovskite nanowires. PNAS, 2016, 113(8): 1993
[9] Zhu H M, Fu Y P, Meng F, et al. Lead halide perovskite nanowire lasers with low lasing thresholds and high quality factors. Nat Mater, 2015, 14(6): 636
[10] Fu Y P Zhu H M Schrader A W, et al. Nanowire lasers of formamidinium lead halide perovskites and their stabilized alloys with improved stability. ACS Nano Lett, 2016, 16(2): 1000
[11] Fu Y P, Meng F, Rowley M B, et al. Solution growth of single crystal methylammonium lead halide perovskite nanostructures for optoelectronic and photovoltaic applications. J Am Chem Soc, 2015, 137(17): 5810
[12] Huang H L, Zhao F C, Liu L G, et al. Emulsion synthesis of size-tunable $CH_3NH_3PbBr_3$ quantum dots: an alternative route toward efficient light-emitting diodes. ACS Appl Mater Interfaces, 2015, 7(51): 28128
[13] Protesescu L, Yakunin S, Bodnarchuk M I, et al. Nanocrystals of cesium lead halide perovskites ($CsPbX_3$, X = Cl, Br, and I): novel optoelectronic materials showing bright emission with wide color gamut. Nano Lett, 2015, 15: 3692
[14] Mali S S, Shim C S, Hong C K, et al. Highly stable and efficient solid-state solar cells based on methylammonium lead bromide ($CH_3NH_3PbBr_3$) perovskite quantum dots. NPG Asia Materials, 2015, 7: e208
[15] Im J H, Lee C R, Lee J W, et al. 6.5% efficient perovskite quantum-dot-sensitized solar cell. Nanoscal, 2011, 3(10): 4088
[16] Huang H, Susha A S, Kershaw S V, et al. Control of emission color of high quantum yield $CH_3NH_3PbBr_3$ perovskite quantum dots by precipitation temperature. Adv Sci, 2015, 2(9): 1500194
[17] Sichert J A, Tong Y, Mutz N, et al. Quantum size effect in organometal halide perovskite nanoplatelets. Nano Lett, 2015, 15(10): 6521
[18] Deng H, Yang X K, Song H S, et al. Flexible and semitransparent organolead triiodide perovskite network photodetector arrays with high stability. Aacs Nano Lett, 2015, 15(12): 7963
[19] Song J Z, Xu L M, Zeng H B, et al. Monolayer and few-layer all-inorganic perovskites as a new family of two-dimensional semiconductors for printable optoelectronic devices. Adv Mater, 2016, 28: 4861
[20] Geim A K, Macdonald A H. Graphene: Exploring carbon flatland. Physics Today, 2007, 23(8): 35
[21] Niu W, Eiden A, Prakash G V, et al. Exfoliation of self-assembled 2D organic-inorganic perovskite semiconductors. Appl Phys Lett, 2014, 104: 171111
[22] Ha S T, Liu X F, Xiong Q H, et al. Synthesis of organic-inorganic lead halide perovskitenanoplatelets: towards high-performance perovskite solar cells. Adv Opt Mater, 2014, 2: 838
[23] Dou L T, Wong A B, Yu Y, et al. Atomically thin two-dimensional organic-inorganic hybrid perovskites. Science, 2015, 349(6255): 1514
[24] Liu J Y, Xue Y Z, Wang Z Y, et al. Two-dimensional $CH_3NH_3PbI_3$ perovskite: synthesis and optoelectronic application. ACS Nano, 2016, 10: 3536
[25] Tao A, Kim F, Hess C, et al. Langmuir-Blodgett silver nanowire monolayers for molecular sensing using surface-enhanced raman spectroscopy. Nano Lett, 2003, 3: 1229
[26] Yang P. Nanotechnology: wires on water. Nature, 2003, 425: 243
[27] Deng H, Dong D D, Qiao K K, et al. Growth, patterning and alignment of organolead iodide perovskite nanowires for optoelectronic devices. Nanoscale, 2015, 7: 4163
[28] Im J H, Luo J S, Franckevicius M, et al. Nanowire perovskite solar cell. Nano Lett, 2015, 15(3): 2120
[29] Zhang D D, Eaton S W, Dou L T, et al. Solution-phase synthesis of cesium lead halide perovskite nanowires. J Am Chem Soc, 2015, 137(29): 9230
[30] Reed M. Quantum dots. Sci Am, 1993, 268(1): 118
[31] Kojima A, Ikegami M, Teshima K, et al. Highly luminescent lead bromide perovskite nanoparticles synthesized with porous alumina media. J Chem Lett, 2012, 41(4): 97
[32] Schmidt L C, Pertegas A, Gonzalez-Carre-Ro S, et al. Nontemplate synthesis of $CH_3NH_3PbBr_3$ perovskite nanoparticles. J Am Chem Soc, 2014, 136(3): 850
[33] Zhang F, Zhong H, Chen C, et al. Brightly luminescent and color-tunable colloidal $CH_3NH_3PbX_3$ (X = Br, I, Cl) quantum dots: potential alternatives for display technology. J ACS Nano, 2015 9(4): 4533
[34] Huang H, Susha A S, Kershaw S V, et al. Control of emission color of high quantum yield $CH_3NH_3PbBr_3$ perovskite quantum dots by precipitation temperature. J Adv Sci, 2015, 2(9): 1500194
[35] Song J Z, Li J H, Li X M, et al. quantum dot light-emitting diodes based on inorganic perovskite cesium lead halides ($CsPbX_3$). Adv Mater, 2015, 27: 7162
[36] Carmona C R, Malinkiewicz O, Soriano, et al. Flexible high efficiency perovskite solar cells. Energy Environ Sci, 2014, 7(7): 994
[37] Eperon G E, Burlakov V M, Snaith, et al. Neutral color semitransparent microstructured perovskite solar cells. ACS Nano, 2014, 8(1): 591
[38] Snaith H J. Perovskites: the emergence of a new era for low-cost, high-efficiency solar cells. J Phys Chem Lett, 2013, 4(21): 3623
[39] Gratzel M, Park N G. Organometal halide perovskite photovoltaics: a diamond in the rough. Nano Brief Rep Rev, 2014, 09(5): 56
[40] Smith I C, Hoke E T, Solis-Ibarra D, et al. A layered hybrid perovskite solar-cell absorber with enhanced moisture stability. Angew Chem Int Ed, 2014, 53: 11232
[41] Park B W, Philippe B, Zhang W L, et al. Bismuth based hybrid perovskites $A_3Bi_2I_9$ (A: methylammonium or cesium) for solar cell application. Adv Mater, 2015, 27: 6806
[42] Cao D H, Stoumpos C C, Farha O K, et al. 2D homologous perovskites as light-absorbing materials for solar cell applications. Am Chem Soc, 2015, 137: 7843
[43] Xing J, Liu X F, Zhang Q, et al. Vapor phase synthesis of organometal halide perovskite nanowires for tunable room-temperature nanolasers. Nano Lett, 2015, 15: 4571
[44] Zhu F, Men L, Guo Y J, et al. Shape evolution and single particle luminescence of organometal halide perovskite nanocrystals. ACS Nano, 2015, 9(3): 2948
[45] Huang M H, Mao S, Feick H, et al. Room-temperature ultraviolet nanowire nanolasers. Science, 2001, 292: 1897
[46] Eaton S W, Lai M L, Gibson N A, et al. Lasing in robust cesium lead halide perovskite nanowires. PNAS, 2016, 113: 1993
[47] Chen S T, Roh K Lee J, et al. A photonic crystal laser from solution based organo-lead iodide perovskite thin films. ACS Nano, 2016, 10: 3959
[48] Tan Z K, Moghaddam S, Lai M L, et al. Bright light-emitting diodes based on organometal halideperovskite. Nat Nanotechnol, 2014, 9(9): 687
[49] Cho H, Jeong S H, Park M H, et al. Overcoming the electroluminescence efficiency limitations of perovskite light-emitting diodes. Science, 2015, 350(6265): 1222
[50] Colvin V L, Schlamp M C, Alivisatos A P, et al. Light-emitting diodes made from cadmium selenide nanocrystals and a semiconducting polymer. Nature, 1994, 370: 354

[51] Gong X W, Yang Z Y, Walters G, et al. Highly efficient quantum dot near-infrared light-emitting diodes. Adv Mater, 2015, 27: 7162

[52] Xing J, Yan F, Zhao Y W, et al. High-efficiency light-emitting diodes of organometal halide perovskite amorphous nanoparticles. ACS Nano, 2016, 10(7): 6623

[53] Yantara N, Bhaumik S, Yan F, et al. Inorganic halide perovskites for efficient light-emitting diodes. J Phys Chem Lett, 2015, 6(21): 4360

[54] Ling Y C, Yuan Z, Tian Y, et al. Bright light-emitting diodes based on organometal halide perovskite nanoplatelets. Adv Mater, 2016, 28: 305

[55] Niu G, Li W, Meng F, et al. Study on the stability of $CH_3NH_3PbI_3$ films and the effect of post-modification by aluminum oxide in all-solid-state hybrid solar cells. Mater Chem A, 2013, 2(3): 705

[56] Abate A, Saliba M, Snaith H J, et al. Supramolecular halogen bond passivation of organic–inorganic halide perovskite solar cells. Nano Lett, 2014, 14(6): 3247